Hydrogen-Bond Interactions between Urethane−Urethane and Urethane−Ester Linkages in a Liquid Crystalline Poly(ester−urethane)

Fu-Sen Yen, Lieh-Li Lin, and Jin-Long Hong*

Institute of Materials Science and Engineering, National Sun-Yat Sen University, Kaohsiung, Taiwan 80424, R.O.C.

Received March 17, 1998; Revised Manuscript Received January 11, 1999

ABSTRACT: Five model compounds (U_u, U_s, DPT, DMT, and MB) and two liquid crystalline poly(ester−urethane)s with inherent urethane and internal and external ester groups were prepared to monitor the hydrogen-bond (H-bond) interactions of urethane−urethane and urethane−ester (including internal and external esters). The model compounds were used to evaluate the extinction coefficient ratios between different free and bonded carbonyl absorption modes in the infrared spectra. The results show extinction coefficient ratios of $\epsilon_{free,u}:\epsilon_{free,ext}:\epsilon_{bonded,ext}:\epsilon_{bonded,u}:\epsilon_{free,int} = 0.84:0.81:0.87:1.23:1.0$. These ratios can then be used to approach mole fractions of different carbonyl groups in the oligomeric and polymeric poly(ester−urethane)s (as PEU-L and PEU-H, respectively) at different temperatures. For both PEU-L and PEU-H, their external ester carbonyl groups can compete efficiently with urethane carbonyl groups for H-bonds at elevated temperatures. Oligomeric PEU-L exhibited a major increase on the external ester carbonyl groups once heated to the mesomorphic state; in contrast, carbonyl variations on PEU-H proceeded in a continuous manner before the isotropization temperature. X-ray diffraction patterns suggest that PEUs form a smectic A layered structure. This result coupled with infrared study provided us the chain conformations of PEUs in their mesomorphic states.

Introduction

Hydrogen-bonding (H-bonding) behavior in polyurethanes has been studied for a long time.[1] Moreover, research on liquid crystalline polyurethanes (LCPUs) was performed frequently in an attempt to disclose the relationship between the H-bond interactions and chain conformation. Previously, several LCPUs had been synthesized basically by two strategies. The first strategy involved the polycondensation reactions between mesogenic diisocyanates and regular diols.[2a−g] The polyurethanes generated from this strategy are either non-LC or LCPUs with high thermal transition temperatures (with high crystal-to-mesophase transition, T_m). Detailed infrared studies on these LCPUs were generally prohibited due to the potential decompositions occurring at high temperatures. The second strategy to synthesize LCPUs concerned the polycondensation reactions of mesogenic diols and aromatic diisocyanate.[3a−n] Among them, LCPUs prepared from 4,4′-bis(6-hydroxyhexoxy)biphenyl (BHHBP) and different aromatic diisocynates (2,4- (or 2,6-)toluene diisocyanate (as 2,4- or 2,6-TDI) or 1,4-phenylene diisocyanate) were studied extensively to explore the bonding conditions of their inherent urethane groups. LCPU prepared from BHHBP and 2,4-TDI has a monotropic mesophase and complicated crystallization behavior.[3j] Two conformations of TDI-derived urethane linkages had been assigned for its bonded carbonyl (−C═O) absorption modes observed in the corresponding infrared (IR) spectra.[3h−m] Due to its symmetrical structure, LCPU synthesized from BHHBP and 2,6-TDI crystallized in its mesophase, and this process was accompanied by a substantial increase of H-bonding as concluded from its IR study.[3n] In both cases, three carbonyl absorption bands attributed to free, ordered, and disordered bonded −C═O groups had been identified and their variations with temperatures studied.

Most reports mentioned above concern polyurethanes with H-bond interactions among urethane groups. Previously, we had prepared four model compounds and two polyurethanes with inherent urethanes and esters[4] and qualitatively characterized the free and H-bonded urethane and esters groups. The results from these two polyurethanes can be correlated with those from the model compounds. However, no quantitative analysis was performed in this study due to the scarcity of extinction coefficient data. Therefore, we wish to further explore this subject in a quantitative manner. For this purpose, liquid crystalline poly(ester−urethane)s of high and low molecular weights (as PEU-L and PEU-H in Scheme 1) with inherent urethane and ester (including internal and external esters) linkages were synthesized by the first strategy prepared from polycondensation reaction of a mesogenic diol (bis[(6-hydroxypentyloxycarbonyl)phenylene] terephthalate (as BHPT in Scheme 1) and 2,4-TDI, and their H-bonding behavior was investigated with Fourier transform infrared spectroscopy (FTIR). In contrast to the LCPUs previously reported,[2,3] PEUs synthesized in our laboratory possess a stable enantiotropic mesophase. The low molecular weight PEU-L has a wide mesophase range between 127 (crystal-to-mesophase transition, T_m) and 193 °C (isotropization temperature, T_i), and for the high molecular weight PEU-H, the corresponding mesomorphic structure can be easily frozen by quenching PEU-H to temperatures below its T_g (∼70 °C). The low thermal transition temperatures for both PEUs enhanced the possibility to characterize their mesophases at low temperatures without the potential decompositions or urethane exchange reactions.

In considering the various H-bond pairs in PEUs (such as urethane−urethane, internal ester−urethane, and external ester−urethane pairs shown in Figure 1), the corresponding carbonyl absorption modes are complicated and difficult to resolve. It is therefore five model

10.1021/ma9804186 CCC: $18.00
Published on Web 04/09/1999

Scheme 1. Syntheses of Mesogenic Diol, BHPT, and Liquid Crystalline Poly(ester−urethane)s (PEUs)

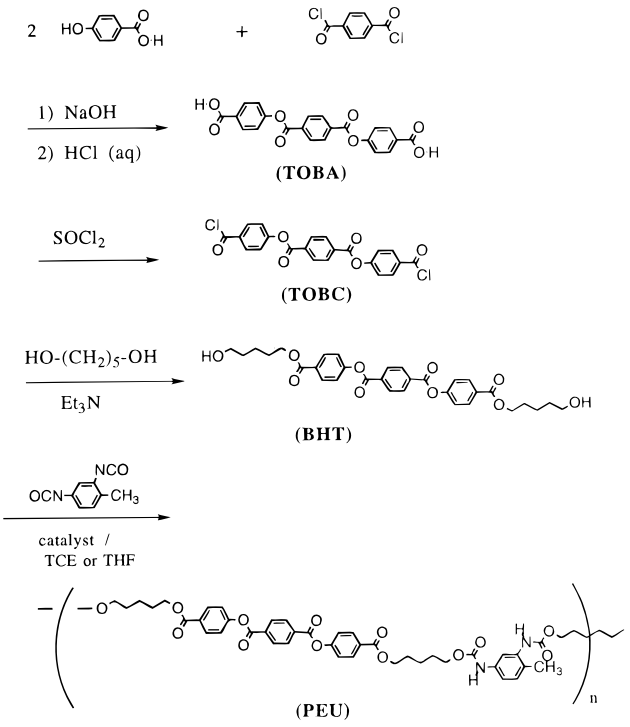

Scheme 2. Structures of Different Model Compounds, DPT, DMT, MB, U_s, and U_u

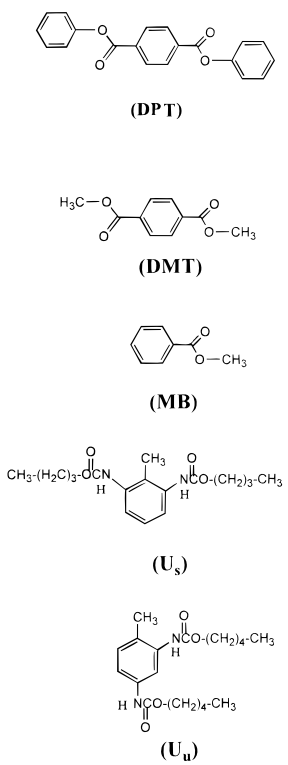

compounds (U_u, U_s, DPT, DMT, and MB in Scheme 2) with similar urethane and ester linkages that are used in this study. With the help of the model compounds, extinction coefficients of the various carbonyl absorption modes can be resolved and used to approach the concentrations of different carbonyl groups in PEU at different temperatures. FTIR was used to resolve the H-bonding behavior at different temperatures. In addition, X-ray diffraction (XRD) patterns at different

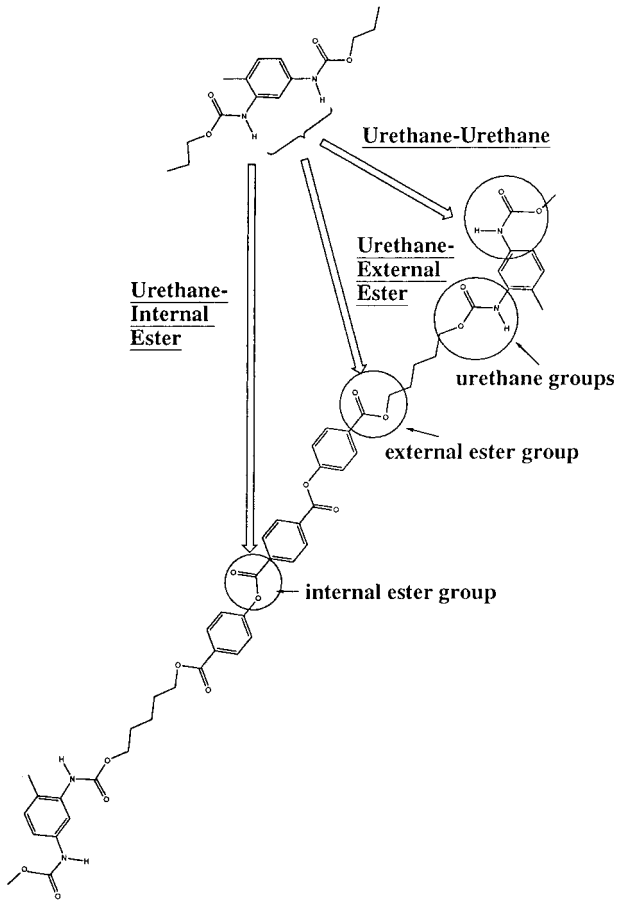

Figure 1. The possible H-bond interaction pairs in PEU.

temperatures were obtained. The conclusions from FTIR and XRD were combined in order to understand the relationship between H-bonding behavior and chain conformation in the mesomorphic state.

Experimental Section

Materials and Instrumentation. Tetrahydrofuran (THF) was distilled from its mixtures with sodium and benzophenone. 1,1,2,2-Tetrachloroethane (TCE) and 1,2-dichloroethane (DCE) were vacuum distilled and stored over 4 Å molecular sieve before use. Benzoyl chloride and terephthaloyl chloride were purified by recrystallization from *n*-hexane. 2,4-TDI and di-*n*-butyltin dilaurate were used without purification.

A Biorad FTS-40 and FTS-155 Fourier transform spectrometer were used in this study. Spectra in the optical range of 4000−400 cm^{-1} were obtained by averaging 64 scans at a resolution of 2 cm^{-1}. Spectra were collected in a vacuum in order to minimize the interference from moisture and oxidative degradation at higher temperatures. A KBr pellet was used for all the solid samples and a liquid cell with a KBr window for liquid ones. Solid mixture of U_s and DPT were first homogeneously mixed through the use of CH_2Cl_2 solvent. The resulting solution was then vacuum distilled to remove the solvent and blended thoroughly with KBr to make the pellet. To analyze the carbonyl absorption, deconvolution and curve fitting were employed to resolve it into several constituents. For a logical approach, the corresponding carbonyl absorption was smoothed and a linear baseline was determined before deconvolution was made. The curve fitting was made on the basis of the following principles: First, the number of the different carbonyl absorption modes was determined based on the possible interaction patterns in the corresponding model compounds and polyurethanes. The band shape of the free and bonded urethane and ester ones were then assumed to be Gaussian. Curving fitting is limited to the spectral data of the carbonyl region between 1770 and 1660 cm^{-1}. The baseline

thus obtained has its two end points removed from the overlapping peak. To ensure a good approximation on the initial values of the chosen parameters, a two-stage fitting process was applied. The procedures afford a best fit of the original curve, and the resulting correlation factors for all the fittings are over 0.995. High-temperature infrared spectra were obtained by placing samples between KBr windows in a homemade steel cell connected to vacuum pump, thermocouples, and temperature sensors.

Proton NMR spectra were recorded with a Varian Fermini-200 200 MHz model. Tetramethylsilane (TMS) was used as internal standard in all cases. The texture of liquid crystals was observed with a Nikon Optiphot-POL microscope equipped with a Linkam TMS controller and a THMS 600 hot stage. Phase transition temperatures were detected with a Perkin-Elmer DSC 7 model. The carrier gas was nitrogen at a flow rate of ca. 10 cm^3/min. Calibration of the calorimeter was conducted for each heating rate using indium and lead standards.

Wide-angle X-ray diffraction for the nonoriented, low molecular weight PEU (PEU-L) was performed with a Siemens diffractometer D 5000 model with Ni-filtered Kα radiation. The system was evacuated to a pressure of 10^{-5} Torr before heating to high temperature. For the oriented, high molecular weight PEU (PEU-H), a Enraf-Nonius 582 D-60 X-ray camera using Cr Kα radiation was used. The oriented specimen was prepared as follows: the PEU-H sample was first heated to 200 °C, and to the resulting isotropic liquid, a pair of treezzer was attached and then quickly withdrawn into a stream of nitrogen gas to prepare an oriented fiber. The collected fibers were then cut into pieces 1 cm long and horizontally aligned before mounting between two spacers. The specimen was then thermally annealed at 90 °C for 36 h to make the final sample. The above procedures were all operated under a nitrogen atmosphere.

Syntheses of U_s, U_u, DPT, DMT, DMT, and BHPT. Syntheses of model compounds U_s, U_u, DPT, MB, and BHPT[5] were synthesized according to the previous procedures.[4] Synthesis of DMT was described below. A solution of terephthaloyl chloride (4.1 g, 20 mmol) in CH_2Cl_2 (20 mL) was slowly added to a vigorously stirred methanol (50 mL, 1.23 mol). The reaction mixture was refluxed for 8 h under a nitrogen atmosphere. The hot solution was filtered, and the filtrate was distilled to remove most of the solvent. The crude product was then dissolved in $CHCl_3$ and subjected to two-phase extraction with aqueous $NaHCO_3$ (pH = 7) once and saturated aqueous NaCl twice. The organic layer was dried over $MgSO_4$ and filtered. The filtrate was concentrated before addition of *n*-hexane to precipitate the crude product. The final product was obtained by operating the same dissolution and precipitation procedures on the crude product. $R_f = 0.81$ (ethyl acetate/*n*-hexane = 1:2 v/v). Anal. Calcd for $C_8H_{10}O_4$: C, 61.58; H, 5.19. Found: C, 61.94; H, 5.07. ^{1}H NMR (200 MHz, $CDCl_3$): δ 7.97 (s, 4 H, aromatic Hs), 3.87 (s, 6 H, $-CH_3$).

Synthesis of Polyurethanes, PEUs. High and low molecular weight PEUs (as PEU-H and PEU-L, respectively) were synthesized by employing different solvents in the preparation step. In the case of PEU-H, 2,4-TDI (3.55 mmol) was dissolved in 5 cm^3 of TCE and then added into a mixture of BHPT (3.45 mmol) in 10 cm^3 of TCE. For preparation of PEU-L, a solution of 2,4-TDI (3.55 mmol) in 5 cm^3 of THF was added slowly into a solution of BHPT (3.45 mmol) in 100 cm^3 of THF. The reaction system was then refluxed for 12 h before being cooled down to room temperature to add catalytic amounts of dibutyltin dilaurate (~0.5 wt %). The reaction was continued for another 36 h. The resulting mixtures were concentrated before the addition of methanol to terminate the reaction. Most of the residual solvents were then evacuated by rotary evaporator. The crude polymer obtained was subjected to Soxhlet extraction by *n*-hexane overnight. The resulting solid was washed with methanol and dried in a vacuum oven at 60 °C overnight to give the final product. η_{inh} (0.10% in TCE, 35°C) = 0.12 dL/g for PEU-L and 0.45 dL/g for PEU-H. The proton NMR (200 MHz, d^6-DMSO) spectrum and the corresponding peak assignments are given in the Discussion section.

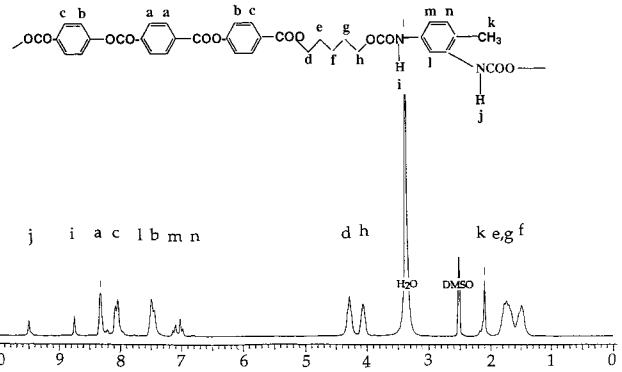

Figure 2. Proton NMR spectrum of PEU-L and the corresponding peak assignments.

Results and Discussion

Synthesis and Characterizations of Poly(ester−urethane). Liquid crystalline poly(ester−urethane)s (PEUs) were prepared by the polycondensation of the mesogenic diol, BHPT, and 2,4-TDI (cf. Scheme 1). BHPT was synthesized by the procedures illustrated in Scheme 1, and the details were given previously.[5] Oligomeric and polymeric PEUs (as PEU-L and PEU-H) were prepared by the use of THF and TCE as reaction solvents, respectively. Since large amounts of THF were needed to dissolve BHPT monomer (for ~2 g of BHPT, 100 mL of THF was required), the corresponding reaction in THF was therefore performed in a rather dilute state. In contrast, BHPT can be easily dissolved in TCE, and this polymerization can be conducted in a more concentrated state as compared to reaction in THF. The difference in the polymerization conditions caused the molecular weight difference on the final products. The inherent viscosity of the low molecular weight PEU-L is pretty low (η_{inh} = 0.12 dL/g), which suggests the oligomeric nature of PEU-L. Distinguished thermal and H-bonding behaviors between oligomeric PEU-L and PEU-H are therefore expected and discussed in a following paper. Due to the oligomeric nature, preparation of PEU-L fiber from its mesomorphic state failed; on the contrary, an oriented fiber of PEU-H sample was specifically prepared for the pinhole X-ray diffraction study.

Proton NMR of PEU-L is shown in Figure 2. The nonequivalency of the urethane −NHs resulted in two different peaks at δ 9.16 and 8.32. The urethane −N*H* ortho to the tolyl methyl group should appear at lower field than the urethane −N*H* at the para position in considering the inductive effect of the methyl group. The protons (a) in the central phenylene ring (−(O═)C−C_4H_4−C(═O)−) have a chemical shift at δ 8.31 while the protons (as b, c) in the neighboring, more e-rich phenylene rings (−O−C_4H_4−C(═O)−O−) show an A_2B_2 pattern at δ 8.08. Comparatively, the protons (m, n) in the TDI-derived phenylene ring have their peak positions lower than the aromatic protons in the ester triads. The TDI-derived phenylene ring is connected to two aliphatic chains by urethane linkages and should be situated in a more e-rich environment as compared to the other phenylene rings, which generally linked with two e-withdrawing ester groups. Other proton assignments for the aliphatic chains are also given in Figure 2. A similar spectrum was resulted for PEU-H and will not be presented here.

Under polarized light, PEU-L exhibited the typical focal conic texture at 165 °C (Figure 3). This texture

Figure 3. Focal−conic textures of PEU-L at 165 °C.

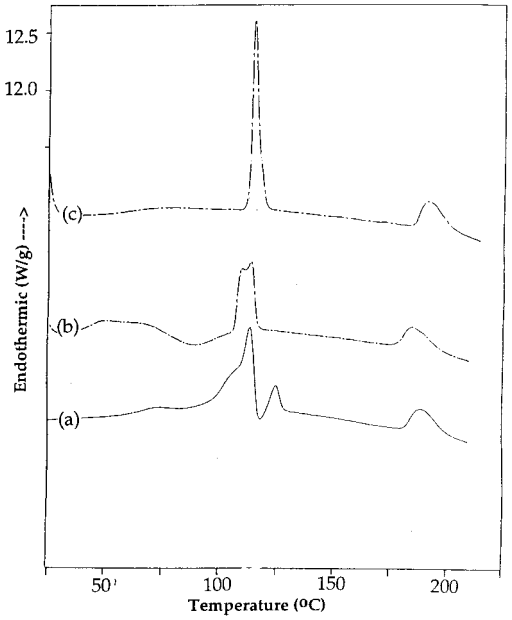

Figure 4. DSC thermograms of PEU-L in (a) the first run, (b) the second run after cooling from 210 °C (isotropic liquid state), and (c) the second heating run after cooling from 210 °C and annealing at 100 °C for 2 h.

can be regenerated in the subsequent cooling from the isotropic liquid state; therefore, an enatiotropic smectic mesophase can be temporarily assigned for the PEU-L. The DSC thermogram of the as-reacted PEU-L in Figure 4a showed a T_g at 70 °C, a multiple melting−recrystallization−remelting transition in the range 80−135 °C, and an endotherm at 189 °C. The second heating after cooling from 210 °C (Figure 4b) showed a T_g at lower temperature than the first heating, a recrystallization exotherm before the double melting peaks, and an endotherm appearing at the same temperature as the first scan (189 °C). The double melting peaks in the second heating run can be altered if the quenched sample was annealed at 100 °C for 2 h. The resulting thermogram (Figure 4c) showed a small glass transition, a sharp melting at 127 °C, and an endotherm appearing at 193 °C. The generation of a sharp crystalline melting and a single endotherm at higher temperatures suggest that thermal treatment increases the conformational regularity and crystallinity; however, the crystallization process during the first and second heating also reflects the fact that chain movement in oligomeric PEU-L proceeds easily at temperatures higher than T_g. Despite

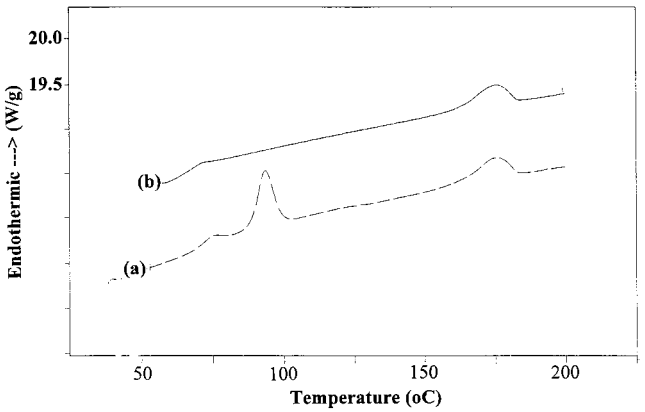

Figure 5. DSC thermograms of PEU−H in (a) the first run and (b) the second run after cooling from 180 °C.

the complicated multiple melting endotherms observed in DSC scans, the POM observation confirms that the first transition in the range of 115 and 127 °C (cf. Figure 4c) corresponds to the transition from crystal to mesophase (T_m) and the second one at around 190 °C as the mesophase to the isotropic liquid state (T_i).

A separate run for the as-reacted PEU-H resulted in a DSC thermogram (Figure 5a) with a T_g at 72 °C and a single melting peak at 91 °C followed by the isotropization transition at 175 °C. The second scan (Figure 5b) after cooling from the isotropic liquid state resulted in a T_g (∼64 °C) at a slightly lower position than first heating and the isotropization transition only. The disappearance of the melting endotherm in the second scan indicates the slow crystallization rate of the polymeric PEU-H, which is distinct from the facile recrystallization process observed for oligomeric PEU-L. Under polarized light, the focal conic texture, once generated, can be easily frozen by the subsequent cooling process. This result was correlated with the DSC scans and reflects the high molecular weight nature of PEU-H.

It is interesting to note that PEU-L has higher thermal transition temperatures (T_m and T_i) than PEU-H does. As cited above, PEU-L is oligomeric in nature (possibly, a few repeat units per polymer chain), and the role of the mesogenic BHPT chain ends on the thermal behavior is especially important for PEU-L. These mobile mesogenic BHPT chain ends in the PEU-L tended to pack into ordered crystalline structure through recrystallization process once PEU-L was heated to temperatures above T_g (as evidenced by the recrystallization exotherms in the DSC thermograms of Figure 4). In contrast, the concentration of the mesogenic BHPT chain ends per polymer chain in PEU-H is conceivably less than those in PEU-L; this factor plus the less mobile chain segments for PEU-H makes its crystallization process inhibited and crystals less perfect than PEU-L. The recrystallization process occurring in PEU-L conceivably increases its T_m transition; also, the higher content of mesogenic chain ends for PEU-L may enhance its mesomorphic order and elevate its T_i transition as compared with PEU-H of less concentration of mesogenic chain ends.

The room-temperature IR spectrum of the as-reacted PEU-L is given in Figure 6. A total of 25 peaks and peak shoulders were assigned (Table 1) from spectral comparisons of other polymers and model compounds with similar chemical groups.[3k,n,6−11] The mesogenic poly-

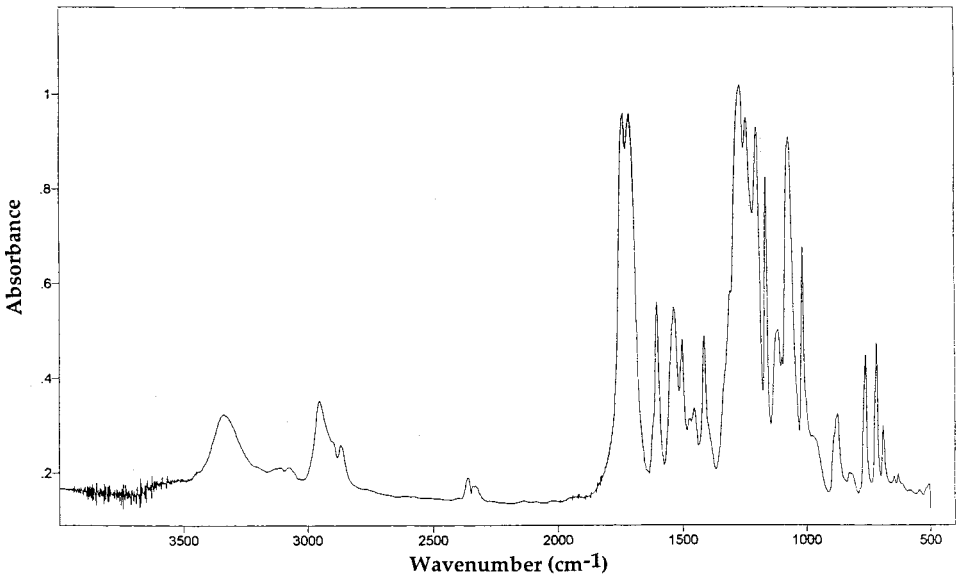

Figure 6. FTIR spectrum of the as-reacted PEU-L at room temperature.

Table 1. Band Assignments for Liquid Crystalline PEU-L

υ (cm^{-1})[a]	intensity[a]	assignment	reference
3410	(w, sh)	free N−H stretching	6, 7
3340	(s)	bonded N−H stretching	6, 7
3119	(vw)	aromatic C−H stretching	8
3070	(w)	aromatic C−H stretching	8
2949	(s)	out-of-phase, asymmetric CH_2 stretching	8
2865	(m)	in-phase, symmetric CH_2 stretching	8
1738	(vvs)	mixed C═O stretching (details in discussion)	
1715	(vvs)	mixed C═O stretching (details in discussion)	
1603	(s)	benzene C−C stretching	3n, 6, 8
1535	(s)	amide II (C−N stretching + N−H bending)	6, 7, 9
1501	(s)	benzene ring C−C stretching (semicircle stretching)	3n, 8
1454	(m)	CH_2 deformation (bending) + in-plane CH_3 bending (in TDI ring)	3n, 6
1412	(s)	benzene C−C stretching	3k, 9
1267	(vvs)	internal C−O stretching (in Ph-*O*−*C*O−Ph)	8
1241	(vvs)	amide III (C−N stretching + N−H bending)	6, 7, 9
1200	(vvs)	C−O−C asymmetric stretching (in Ph-*O*−*C*O−Ph)	7, 9
1161	(vs)	CH in-plane bending	3k
1112	(s)	C−O−C asymmetric stretching (in R-*O*−*C*O−Ph)	7, 9
1071	(vvs)	C−O−C asymmetric stretching (in -*O*−*C*O−NH)	7, 9
1014	(vs)	C−O deformation (wagging)	10
872	(m)	out-of-plane C−H bending	11
761	(s)	out-of-plane C−H deformation (adjacent to −O-) + -CO−O− out-of-plane bending	6, 8
717	(s)	out-of-plane C−H deformation (adjacent to C═O) + out-of-plane NH wagging	3n, 8
691	(m)	out-of-plane −C═O deformation	8

[a] υ = frequency; s = strong, m = medium, w = weak, sh = shoulder, v = very.

urethanes prepared from BHHBP and 2,4-TDI, which stands for the monosubstituted 2,4-phenylene diisocyanate, aid in the vibration peak assignments for the moiety derived from 2,4-TDI. For the assignments of the external and internal ester groups, the previous infrared study on a liquid crystalline compound, $CH_3(CH_2)_9$−OOC−C_6H_4−OOC−C_6H_4−COO−C_6H_4−COO−$(CH_2)_9$−CH_3, provides fruitful information.[8] In considering the various possible urethane−urethane and ester−urethane interactions, the −NH (3500−3350 cm^{-1}) and −C═O (1740−1690 cm^{-1}) absorption bands are broad due to the presence of different stretching modes.

IR study on the −NH and −C═O regions provides a powerful method to evaluate the conformation change of urethane polymers. Temperature-programmed IR spectra of PEU-L and PEU-H in the −NH and −C═O absorption regions were given in Figures 7 and 8, respectively. For PEU-L, the band maximum of the −NH stretching is centered at around 3350 cm^{-1} (the small peak at 3445 cm^{-1} is due to the overtone of the carbonyl absorption) at 25 and 50 °C. As the temperature was increased (as in the cases of 110 and 155 °C), the band maxima were shifted to lower frequencies. This frequency shift may be associated with the recrystallization process occurring at temperatures above T_g and/or the imposing of orientation order upon transformation into a mesomorphic state. In both states, the −NHs would bond to either the urethane or ester −C═O groups in a more efficient manner as compared to the solid glassy state. As temperatures were further increased (i.e., at 180 and 200 °C), the band maxima were shifted to the higher frequencies. At 200 °C, a left shoulder attributed to the free −NH absorption appeared at around 3407 cm^{-1}. This frequency shift, which corresponds to a reduction on the average strength of the H-bonds, and the emergence of the free −NH absorption band indicate the formation of a less ordered structure in the isotropic liquid state of PEU-L. For

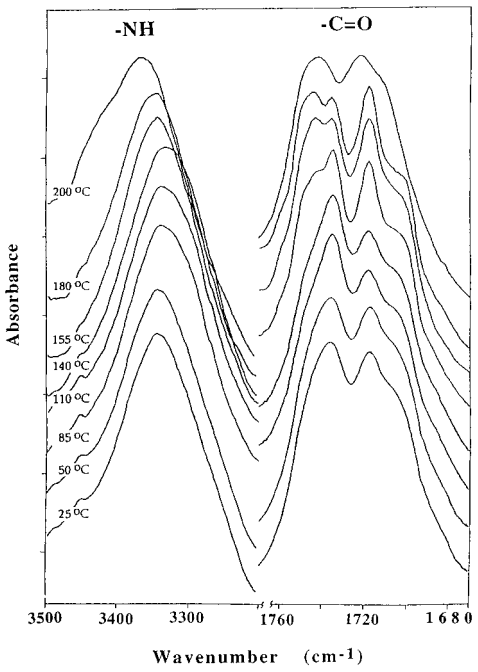

Figure 7. FTIR spectra in the N−H and −C═O stretching regions for PEU-L at different temperatures.

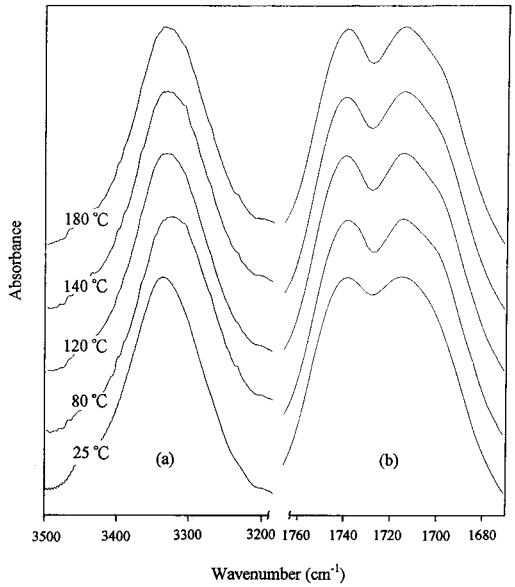

Figure 8. FTIR spectra in the N−H and −C═O stretching regions for PEU-H at different temperatures.

PEU-H, the −NH stretchings at 3335 cm^{-1} shifted to lower frequency if PEU-H was heated from 25 to 80 °C (above T_g). From 80 to 180 °C (during isotropization), the −NH stretching showed a similar shift to higher frequencies as PEU-L does; however, the magnitude of frequency shift is larger for PEU-L ($\Delta\upsilon \sim 25$ cm^{-1} from 85 to 180 °C) as compared to PEU−H ($\Delta\upsilon \sim 13$ cm^{-1} from 80 to 180 °C). The larger frequency shift also reflects much drastic changes in the shapes of the −C═O absorption bands for PEU-L (Figure 7) as compared to PEU-H. For PEU-L, the −C═O absorption modes consist of two broad bands with a right shoulder at 25 °C. Upon heating to high temperatures (≤180 °C), we observed the gradual intensity increase of the right band and the development of a new absorption peak at the high-frequency region. Further heating to 200 °C resulted in a similar two-band shape as in the case of 25 °C, but a detectable frequency shift was noticed. Comparatively, the −C═O absorption modes for PEU-H (Figure 8) varied insignificantly with temperature. The two broad bands observed at 25 °C changed slightly with temperature, and quantitative results can only be obtained from the deconvolution and curve-fitting procedures described below. Here, primary comparison between Figures 7 and 8 also suggests the oligomeric nature of PEU-L due to its significant alternations of the carbonyl absorption modes with temperatures.

Unlike the −C═O absorption modes, the −NH stretchings generally have a strong dependence of their extinction coefficients upon absorption frequencies, and this results in the conformational insensitivity of the −NH absorption.[12−15] To have a quantitative result, we had to concentrate our analysis on the −C═O absorption region.

As expected, the appearance of the −C═O absorptions is complicated due to the different carbonyl groups present in PEU-L. Previously, we had prepared different model compounds with inherent urethanes and esters (including internal and external esters), and their corresponding −C═O absorption bands were studied.[4] With information from the previous study, we can resolve the −C═O absorptions into six bands, which are attributed to the free internal ester (−C═$O_{free,int}$; 1740−1735 cm^{-1}), the free urethane (−C═$O_{free,u}$; 1736−1728 cm^{-1}), the free external ester (−C═$O_{free,ext}$; 1725−1722 cm^{-1}), the disordered bonded urethane (disordered −C═$O_{bonded,u}$; 1718−1714 cm^{-1}), the bonded external ester (−C═$O_{bonded,ext}$; 1710−1706 cm^{-1}), and the ordered bonded urethane (ordered −C═$O_{bonded,u}$; 1702−1692 cm^{-1}) −C═O groups. With the known numbers of the possible carbonyl absorption modes in PEUs, the broad carbonyl peaks in Figure 6 were subjected to deconvolution and curve-fitting procedures. The procedures of deconvolution and curve fitting were detailed in the Experimental Section, and their reliability will be discussed below.

The summarized results in Table 2 show variations of frequencies and the calculated molar fractions of different carbonyl absorption groups at different temperatures. Several preliminary observations can be given before further quantitative analysis. First, no bonded internal ester is assigned in Table 2 since the previous study[4] suggested that the internal ester −C═O groups are incapable of bonding with the urethane −NHs due to the steric bulkiness. Also, the resolved concentration of the −C═$O_{free,int}$ groups at any temperatures below 200 °C remains relatively constant. This suggests that the internal ester groups are inert to thermal agitation if we assume the corresponding extinction coefficients at different temperatures are the same. Second, the resolved peak maxima of the different carbonyl absorption bands coincide reasonably with those determined previously[4] from model compounds (compounds referred to here are exactly the same as we used in this study). The study on the mode compound U_u suggested that the peak frequency of the ordered −C═$O_{bonded,u}$ absorption ranged from 1695 to 1699 cm^{-1} depending on its thermal history. PEU-L has its ordered −C═$O_{bonded,u}$ absorption bands all located at 1700 cm^{-1}, a frequency higher than those at 1695 cm^{-1} for PEU-H. The frequency difference may reflect the relative H-bonding strength between PEU-L and PEU-H and will be discussed below. Despite the slight difference,

Table 2. Frequency and the Calculated Molar Fractions of the Carbonyl Modes at Different Temperatures

	urethane −C═O				external −C═O				internal −C═O			
	ordered		disordered		free		bonded		free		free	
T^a	τ^b	$X_{\text{bonded,u}}{}^c$	τ^b	$X_{\text{bonded,u}}{}^d$	τ^b	$X_{\text{free,u}}{}^e$	τ^b	$X_{\text{bonded,ext}}{}^f$	τ^b	$X_{\text{free,ext}}{}^g$	τ^b	$X_{\text{free,int}}{}^h$
a. Oligomeric PEU-L Sample												
25	1700	9.4	1716	13.8	1733	9.9	1708	14.7	1724	19.1	1742	33.2
50	1700	9.4	1716	13.6	1733	10.7	1708	14.7	1724	18.2	1742	33.3
85	1700	8.0	1716	14.0	1733	11.1	1708	14.5	1724	19.1	1742	33.3
110	1700	7.8	1717	13.9	1733	11.4	1708	14.5	1724	18.9	1743	33.5
140	1699	6.8	1718	14.1	1733	13.1	1707	20.7	1725	12.4	1744	33.0
155	1699	6.2	1717	14.1	1733	13.8	1708	20.0	1725	12.5	1743	33.4
180	1700	5.9	1718	14.0	1733	13.7	1708	20.0	1725	13.5	1745	32.9
200	1699	5.7	1717	11.0	1735	16.1	1706	16.9	1726	17.0	1745	33.2
b. Polymeric PEU−H Sample												
25	1695	18.1	1716	10.7	1734	5.3	1706	15.3	1725	17.4	1743	33.2
80	1695	14.0	1716	10.1	1734	9.0	1706	18.5	1725	14.7	1743	33.8
120	1695	11.5	1716	14.7	1734	9.4	1706	18.7	1725	13.3	1743	32.3
140	1695	10.8	1716	11.9	1734	8.9	1706	21.3	1725	13.2	1743	34.0
180	1695	11.9	1716	8.4	1734	13.2	1706	17.8	1725	14.5	1743	34.1

[a] Temperature, °C. [b] Peak frequency of the resolved band, cm^{-1}. [c] Molar fraction of the ordered bonded urethane, %. [d] Molar fraction of the disordered bonded urethane, %. [e] Molar fraction of the free urethane, %. [f] Molar fraction of the bonded external ester, %. [g] Molar fraction of the free external ester, %. [h] Molar fraction of the free internal ester, %.

both polymers have their ordered $-C{=}O_{\text{bonded,u}}$ absorption frequency correlated with the previous study. Third, the relative amounts of $-C{=}O_{\text{free,ext}}$ and $-C{=}O_{\text{bonded,ext}}$ groups showed major variations once PEU-L was heated from 110 to 140 °C (mesomorphic state); however, both groups in PEU-H exhibited slight changes upon transformation to the mesophase (from 80 to 120 °C). Fourth, isotropization caused an increase of the free carbonyl (including free external ester and free urethane) groups at the expense of total bonded urethane (including ordered and disordered) and bonded exteranl ester carbonyl groups.

Model Compounds Study. For a quantitative analysis, extinction coefficients (ϵ's) of different carbonyl modes are basically needed. Therefore, model compounds inherent with the characteristic urethane and ester carbonyl linkages are used in this study to evaluate the ϵ values. Model compounds (U_u, U_s, DPT, and MB in Scheme 2) with specific carbonyl groups had been previously prepared in our laboratory.[16] The ϵ values of the $-C{=}O_{\text{free,int}}$ and $-C{=}O_{\text{free,ext}}$ absorption modes can be obtained by measuring the carbonyl bands of DPT and MB, respectively. According to our previous study,[4] the symmetric U_s is highly crystalline, and its inherent urethane carbonyl groups are completely bonded to the its urethane −NH; therefore, the $-C{=}O_{\text{bonded,u}}$ absorption can be evaluated by the use of the solid U_s. In contrast, unsymmetric U_u has high portions of nonbonded carbonyl groups, and its solution IR spectra can be used to approach the ϵ value of the free urethane absorption. In any event, the most difficult task would be the measurement for the $C{=}O_{\text{bonded,ext}}$ absorption since formation of bonded external carbonyl groups is accompanied by the generation of the $-C{=}O_{\text{bonded,u}}$ groups, also. To exclude the possibility to form $-C{=}O_{\text{bonded,u}}$ groups, a mixture solution of small amounts of U_u in liquid MB was used. Due to the low content (5−15 wt %) of the U_u compound in MB, the urethane carbonyl in U_u would only form H-bonds to the surrounding MB molecules and not bond to any U_u to yield bonded urethane groups. Since two compounds were used here, and for the sake of standardization, mixtures of model compound pairs were prepared in this research to obtain the relative extinction coefficient ratios (instead of absolute extinction coefficient). As suggested above, the internal ester −C═O group is inert to the urethane −NH, and the corresponding peak areas at different temperatures are almost the same; therefore, the $-C{=}O_{\text{free,int}}$ group in DPT was considered to be an internal standard for the other −C═O absorption modes.

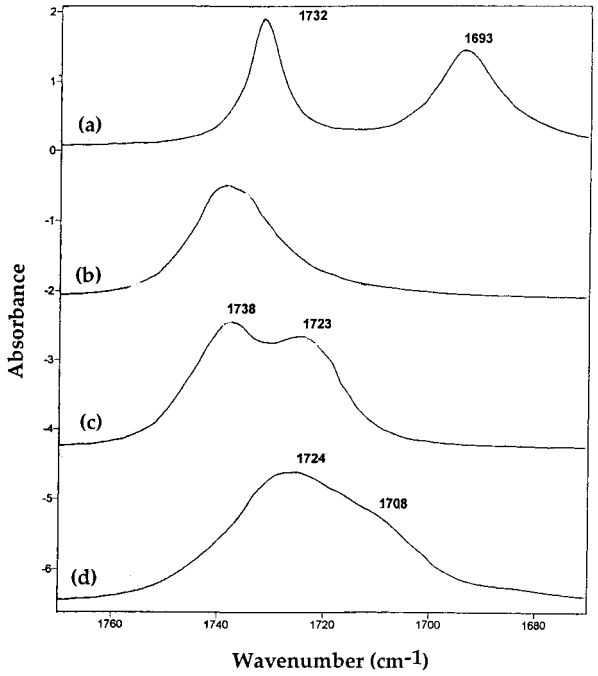

Figure 9. FTIR spectra of model compound pairs of (a) U_s/DPT (KBr pellet), (b) U_u/DPT (in DCE), (c) DMT/DPT (in DCE), and (d) U_u/MB (the molar ratio of model compounds used in each pair is 1:1).

The −C═O absorption patterns from different mixture pairs were selectively shown in Figure 9. The solid U_s/DPT mixture (Figure 9a) of 1/1 molar ratio was used to approach the ϵ ratio between the $-C{=}O_{\text{bonded,u}}$ and $-C{=}O_{\text{free,int}}$ modes. The appearance of two Gaussian-shaped peaks indicates the H-bond interaction between internal ester −C═O in DPT and urethane −NH in U_s is absent, an observation that had been made in our previous study.[4] This conclusion can also be supported by the fact that no peak other than the $-C{=}O_{\text{bonded,u}}$ and $-C{=}O_{\text{free,int}}$ bands is present. In contrast to the

solid-state analysis, the H-bond interactions should be negligible if concentration of the urethane solute is small; therefore, a dilute (∼4 wt % for each solute) solution of U_u and DPT in DCE was used to simulate the $-C{=}O_{free,u}$ and $-C{=}O_{free,int}$ modes. The resulting carbonyl absorption pattern of the U_u/DPT (1:1 molar ratio) mixture in DCE (Figure 9b) is broad and unsymmetric in shape and was deconvoluted to two bands centered at 1745 and 1732 cm^{-1}. The location of the $-C{=}O_{free,u}$ band at 1732 cm^{-1} is consistent with our previous results;[4] however, the $-C{=}O_{free,int}$ band in this case locates at higher frequency than our previous result (1740−1735 cm^{-1}) obtained from solid model compounds. This difference can be clarified by our previous study on bis[4-(pentyloxycarbonyl)phenylene] terephthalate) (BPT).[5] The $-C{=}O_{free,int}$ absorption for the solid BPT appeared at 1723 cm^{-1}, but for BPT in $CHCl_3$, a 1743 cm^{-1} peak was resolved. The frequency difference indicates a change in the conformation of the internal −O−Ar− bonds. Similarly, carbonyl absorption modes for a DMT/DPT mixture in 1,2-dichloroethane (DCE) (Figure 9c) can be used to confirm the $-C{=}O_{free,ext}$ and $-C{=}O_{free,int}$ bands (at 1738 and 1723 cm^{-1}, respectively). Comparatively, a U_u/MB mixture possesses two H-bonding pairs instead of a single H-bond interaction involved in the above three cases (mixtures of U_s/DPT, U_u/DPT, and DMT/DPT). To eliminate the possible urethane−urethane interaction, concentrations of U_u in MB were limited in the range 5−15 wt %. Due to the low U_u concentrations, the H-bonding between U_u molecules should be negligible, and the −NH groups in U_u can only be bonded to the surrounding −C═O groups in MB. The −C═O absorption pattern in Figure 9d can be reasonably resolved into three bands attributed to the $-C{=}O_{free,u}$ (1738 cm^{-1}), $C{=}O_{bonded,ext}$ (1726 cm^{-1}), and $-C{=}O_{bonded,ext}$ (1708 cm^{-1}) modes.

According to the Beer−Lambert law, the relative peak areas (A_i/A_j) are equal to $(\epsilon_i/\epsilon_j)(c_i/c_j)$ (where $c_{i,j}$ is the concentration of the specific carbonyl species i (or j)) if a constant specimen thickness was applied in each experiment. The relative extinction coefficient, ϵ_i/ϵ_j, was then obtained easily since equal molar ratios were applied in each mixture pair used in this study. For a solid U_s/DPT mixture, the concentration unit is referred to as the grams of KBr used in the solid pellets. However, special care should be taken to prepare solid pellets of constant thickness. In summary, the relationship between various extinction coefficients is $\epsilon_{free,u}$:$\epsilon_{free,ext}$:$\epsilon_{bonded,ext}$:$\epsilon_{bonded,u}$:$\epsilon_{free,int}$ = 0.84:0.81:0.87:1.23:1.0. The absolute values for various ϵ_s can be obtained by the ϵ value of the $-C{=}O_{free,int}$ absorption (=12.4 × 10^3 L/mol/cm^3) measured from the dilute solution of DPT in DCE.

Previously, several reports had disclosed a value of the $\epsilon_{bonded,u}/\epsilon_{free,u}$ in the range 1.05−1.8.[16−18] Our value of $\epsilon_{bonded,u}/\epsilon_{free,u}$ (=1.46) reasonably falls in the reported ranges. Unfortunately, the reported extinction coefficient ratios between free and bonded esters are all aimed at the interactions between esters and phenolic hydrogen ($-C_6H_4-OH$);[19,20] therefore, no comparison can be made at the present time. The same situation is met in considering the interactions between ester and urethane.

Quantitative Analysis of the −C═O Absorptions of PEUs. The relative ϵ values obtained from model compounds can be used to analyze the carbonyl absorption bands of PEUs at different temperatures. However, certain assumptions should be made before the results from model compounds can be applied to the polymer case. First, extinction coefficients of different carbonyl modes are independent of temperature. This assumption had been previously made for other polyurethane systems.[12] Second, ϵ values of the ordered and disordered $-C{=}O_{bonded,u}$ groups are assumed to be the same in this study. This assumption deviates from the real situation and is made for the sake of simplification. With this premise, the ϵ value obtained from U_s was used to represent all the ordered and disordered $-C{=}O_{bonded,u}$. Third, the dependence of extinction coefficient on its located frequency is neglected; a supposition was also made on the study of other polyurethane systems.[12]

The limitations of the curve-fitting method should be discussed beforehand. As concluded by Maddams,[21] the number of component peaks in a composite profile and their half-widths are the two most critical variables in the curve-fitting process. The number of component peaks can be reasonably determined on the basis of the possible interactions between urethane−urethane and urethane−ester in the present system. However, peak widths are generally difficult to resolve. For a satisfactory approach to peak width, reasonable optimization on other fitting parameters such as baseline and peak shape is necessary. In our procedure, a Gaussian peak profile was used since the choice of Lorentzian peak shape is usually not good for solving a system consisting of closely overlapping peaks. Here, a simple linear baseline was used with its two end points removed from any overlapping peak. Also, the linear baseline can be precisely determined by several adjustment steps to an extent that the molar fractions of the internal ester approach the theoretical value of $^1/_3$ (again, use of an internal ester as internal standard is based on its ineptness toward H-bonding and thermal agitation). With the appropriate choices of parameters for curve fitting, peak areas can be used to evaluate the molar fractions of different carbonyl groups, and the results are listed in Table 2. At this moment, we would be skeptical about the curve-fitting results since certain resolved peaks (e.g., ordered $-C{=}O_{bonded,u}$ and $-C{=}O_{bonded,ext}$) are strongly overlapped. Nevertheless, in addition to the theoretical value of the internal ester group, another criterion concerning the theoretical amounts of the inherent carbonyl groups can also be used to test the validity of the curve-fitting results. The total molar fractions of external ester (= $X_{total,ext}$ = $X_{free,ext} + X_{bonded,ext}$) and urethane groups ($X_{total,u} = X_{free,u} + X_{bonded,u}$) are summarized in Table 3, which indicates molar fractions of both carbonyl groups approach the theoretical value of $^1/_3$. This result may suggest that the curve-fitting results for the present system are within a reasonable range.

The calculated molar fraction (X_i) of various −C═O absorption modes for PEU-L and PEU-H were plotted as a function of temperature in Figures 10 and 11, respectively. For PEU-L, the first noticeable feature in Figure 10 is the relatively constant values of $X_{free,int}$s and disordered $X_{bonded,u}$s (∼14%) at temperatures below 200 °C (isotropization temperature). Except the $-C{=}O_{free,int}$ and the disordered $-C{=}O_{bonded,u}$, other four carbonyl ($-C{=}O_{free,u}$, $-C{=}O_{free,ext}$, $-C{=}O_{bonded,ext}$, and the ordered $-C{=}O_{bonded,u}$) modes showed certain variations in their molar fractions as PEU-L was heated to high temperatures. Among them, the $-C{=}O_{free,ext}$ and $-C{=}O_{bonded,ext}$ bands exhibited major changes as PEU-L

Table 3. Molar Fractions of Different Carbonyl Groups Calculated from Curve-Fitting Results

temp (°C)	$X_{int,Es}$ (%)	X_u (%)[a]	$X_{ext,Es}$ (%)[b]
	a. PEU-L Sample		
25	33.20	33.02	33.78
50	33.26	33.69	33.06
85	33.30	33.10	33.60
110	33.50	33.15	33.36
140	33.01	33.94	33.05
155	33.40	34.09	32.51
180	32.91	33.63	33.47
200	33.19	32.89	33.92
	b. PEU−H Sample		
25	33.15	34.13	32.71
80	33.78	33.08	33.14
120	32.33	35.66	32.00
140	33.97	31.53	34.49
180	34.13	33.50	31.01

[a] X_u is total molar fractions of ordered, disordered bonded, and free urethane carbonyl groups [b] $X_{ext,Es}$ is total molar fractions of bonded and free external carbonyl groups.

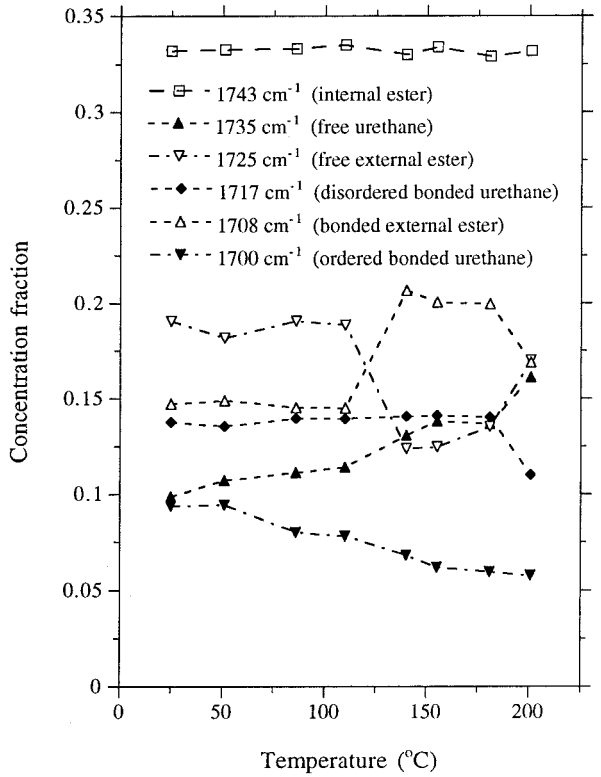

Figure 10. Calculated molar fractions (X_i) of various −C═O absorption groups in PEU-L at different temperatures.

was transformed from a solid to mesomorphic state. When heated from 110 to 140 °C, $X_{free,ext}$ decreased from 18.8 to 12.4% and the $X_{bonded,ext}$ increased from 14.5 to 20.7%. This concentration change caused alternation on the relative molar fractions between the ordered −C═$O_{bonded,u}$ and −C═$O_{free,u}$. (The molar fractions of the disordered −C═$O_{bonded,u}$ are relatively constant as compared to the ordered −C═$O_{bonded,u}$.) It is suggested that the external ester carbonyl groups in PEU-L would compete with the urethane carbonyls for H-bonding once PEU-L was transformed from the solid to the liquid mesomorphic state. Concentrations of all carbonyl groups remained relatively constant in the mesomorphic state (between 140 and 200 °C). In the isotropic liquid state, we observed the decreases of the −C═$O_{bonded,ext}$ and the disordered −C═$O_{bonded,u}$ and the increases of the −C═$O_{free,ext}$ and the −C═$O_{free,u}$ groups. This observation is reasonable considering that isotropization disrupts the orientation order in the mesomorphic state.

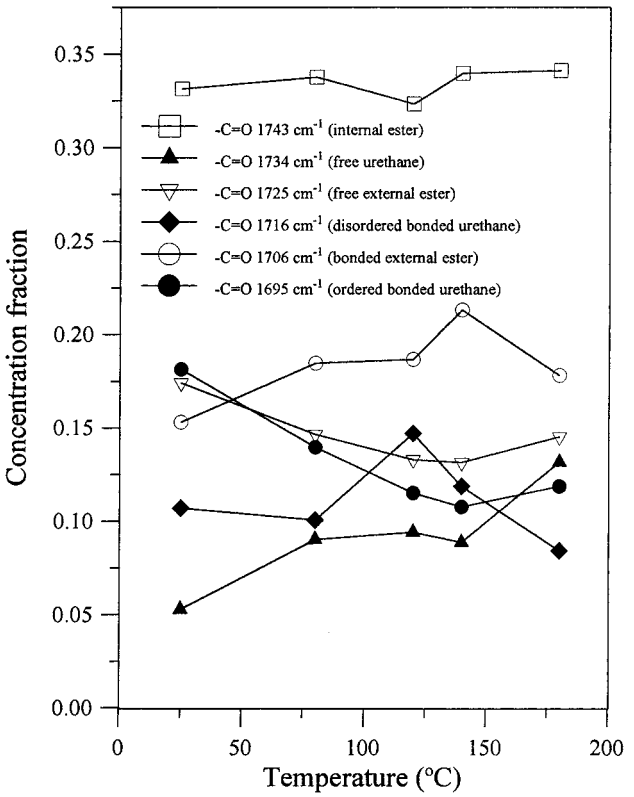

Figure 11. Calculated molar fractions (X_i) of various −C═O absorption groups in PEU-H at different temperatures.

Similar to the case of PEU-L, the concentration of the −C═$O_{free,int}$ group for PEU-H remained constant at temperatures below 180 °C (Figure 11). Another similar feature is the continuous increase of the −C═$O_{bonded,ext}$ group at the expense of the ordered −C═$O_{bonded,u}$ groups at temperatures below T_i (∼180 °C). This phenomenon was also observed in PEU-L sample and attributed to the competition between the external ester and urethane carbonyl groups for the urethane −NH. Despite the above similar points, certain dissimilarities due to the molecular weight difference between PEU-L and PEU-H do exist. First, the initial ordered $X_{bonded,u}$ (=18.1%) for PEU-H is higher than that for PEU-L (=9.4%). It is suggested that PEU-H may contain certain ordered domains due to its polymeric nature, and enhanced H-bond interactions between urethane groups may be expected in these ordered domains. The ordered −C═$O_{bonded,u}$ group for PEU-H is located at a lower position of 1695 cm^{-1} as compared to 1700 cm^{-1} for PEU-L, which indicates that the average H-bonding distance and strength of urethane groups for PEU-H may be shorter and stronger than those for PEU-L. Second, except for the disordered −C═$O_{bonded,u}$, other carbonyl groups showed little alternations from solid to the mesomorphic state (80 to 120 °C). For the oligomeric PEU-L, major variations on the −C═$O_{bonded,ext}$ and −C═$O_{free,ext}$ groups can be rationalized in terms of the enhanced segmental mobility from solid to the liquid mesomorphic states. In contrast, the polymeric nature of PEU-H may make its mesomorphic state more viscous than PEU-L; therefore, variations in the segmental mobility and thus the molar ratios of different carbonyl groups proceeded in a less drastic manner than PEU-L

Table 4. Comparison between the Bonded Ester and Urethane Groups at Different Temperatures

temp (°C)	mol fractions of bonded urethane carbonyls[a] (%)	mol fractions of bonded ester carbonyls[b] (%)
	a. PEU-L Sample	
25	23.1	14.7
50	23.0	14.9
85	22.0	14.5
110	21.7	14.5
140	20.8	20.7
155	20.3	20.0
180	20.0	20.0
200	16.8	16.9
	b. PEU-H Sample	
25	28.8	15.3
80	24.1	18.5
120	26.3	18.7
140	22.7	21.3
180	20.3	17.8

[a] Referred to the total molar fractions of ordered and disordered bonded urethane. [b] Referred to the molar fraction of the bonded external esters.

does. In the mesophase (from 120 to 140 °C), detectable concentration changes are the increase of the $-C{=}O_{bonded,ext}$ group at the expense of the disordered $-C{=}O_{bonded,u}$ group, a result attributable to the competition between urethane and external ester carbonyl groups. Upon heating to the isotropic liquid state (180 °C), we observed the increase of free carbonyl absorption modes ($-C{=}O_{free,u}$ and $-C{=}O_{free,ext}$) accompanied by the decrease of the total $-C{=}O_{bonded,u}$ (here, the slight increase of the ordered $X_{bonded,u}$ was compensated by the large decrease of the disordered $X_{bonded,u}$) and $-C{=}O_{bonded,ext}$ groups.

The competition between external ester and urethane groups can be verified by comparison between the molar fractions of the total bonded urethanes (including ordered and disordered urethanes) and bonded external esters at different temperatures (as shown in Table 4). At temperatures below 140 °C, PEU-L contained more bonded urethanes (molar fractions >20%) than the bonded external esters; however, as PEU-L was transformed into the mesomorphic state (in the temperature range of 110 and 180 °C), the molar fractions of the bonded external esters increased to an extent approximately equivalent to that of the bonded urethanes. For polymeric PEU-H, similar concentration variations on the total bonded urethane and bonded external esters were observed. As reported by Boyarchuk et al.,[22] the bonding abilities between urethane and ester groups can be evaluated from the infrared spectra of *N*-phenylethylurethane, $Ph{-}NH{-}C(=O){-}O{-}C_2H_5$ (NU), and its mixtures with other ester compounds in a neutral solvent CCl_4. The bonded −NH stretching for pure NU solution appears at 3345 cm^{-1}, but upon the addition of dimethyl adipate, the −NH stretching shifts to a higher position of 3363 cm^{-1}. This result suggests that ester compounds (such as dimethyl adipate) can bond to the urethane −NH efficiently in the presence of urethane −C═O. Also, on the basis of the study on polymeric systems, Boyarchuk concluded that the predominant formation of one or another of H-bond will depend mainly on the relative concentrations of the different proton-acceptor groups (i.e., urethane and ester carbonyl groups) and on the spatial arrangement in the polymer chain. For our present case, the frozen chain arrangements in the solid state limited the external esters to bond to urethane −NHs; but once the chains were transformed into the more mobile mesomorphic state, the external ester −C═O group can bond to −NH as effectively as the urethane −C═O group. This bonding situation surely relates to the chain conformation in the mesomorphic state, a point that will be further discussed below.

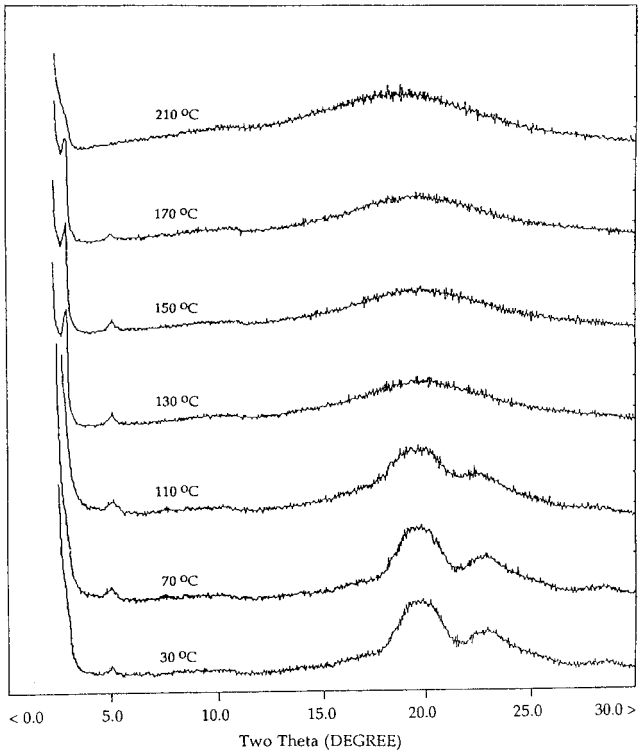

Figure 12. Wide-angle X-ray diffraction (XRD) patterns of the nonoriented PEU-L at different temperatures.

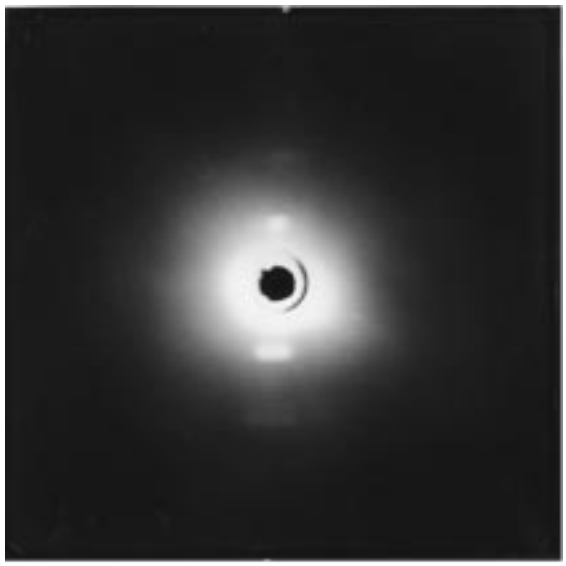

Figure 13. Pinhole X-ray photograph of the oriented PEU-H.

Wide-Angle X-ray Diffraction. Wide-angle X-ray diffraction (XRD) patterns of the nonoriented PEU-L are shown in Figure 12. At lower temperatures (i.e., 30, 70, and 110 °C), all the diffraction profiles show the presence of a small peak around $2\theta \sim 5°$ and two major, intense peaks around $2\theta = 22°$ and 24°. These two intense peaks in the wide angle region are broad in shape and correspond to certain ordered structures in the solid state. As PEU-L was further heated to 130 °C,

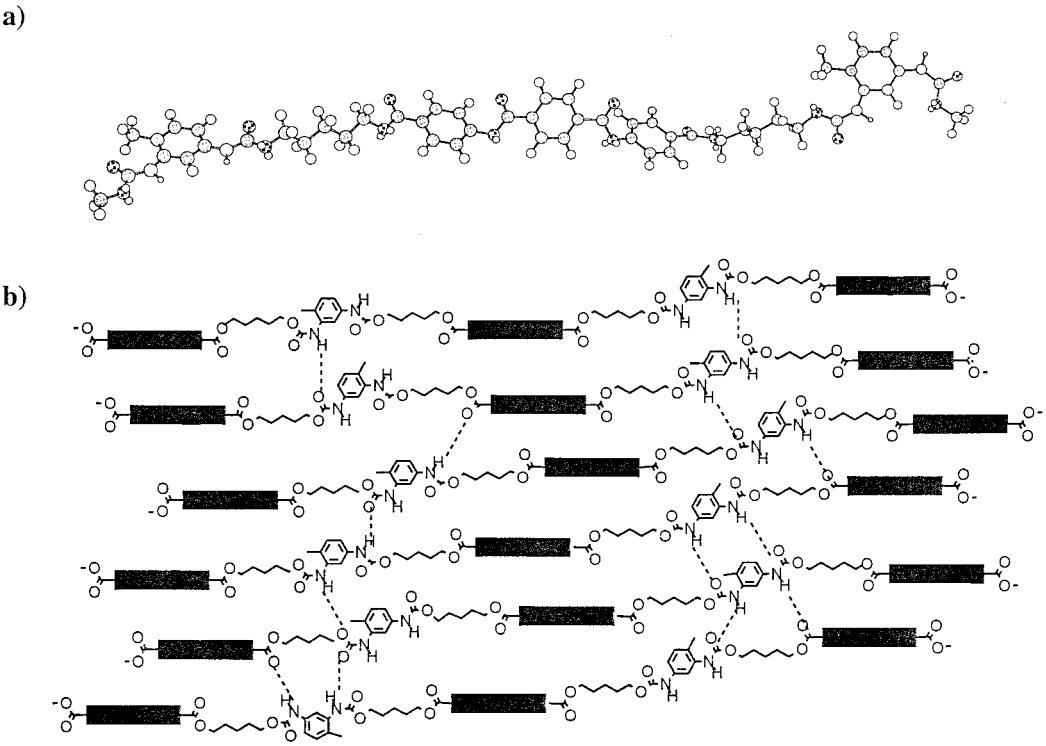

Figure 14. (a) Model structure of monomeric unit of PEU (plus next 2,4-TDI unit); repeat length is 41.1 Å. (b) Proposed imperfect smectic layer structure for PEU.

these two peaks merged into one (peak centered at $2\theta \sim 21.8°$, corresponding to an average intermolecular distance of 4.5 Å), and an extra peak started to appear at $2\theta = 2.6°$ (=36.7 Å; the one at $2\theta = 5.4°$ (=18.1 Å) is the corresponding second-order diffraction peak). The existence of the low-angle diffraction peak indicates formation of a smectic mesophase. After isotropization (i.e., at 210 °C), the two peaks in the low angle region disappeared, and the broad, high angle peak remained the same as it was in the mesomorphic state.

Room-temperature X-ray diffraction study was performed on an oriented, high molecular weight sample of PEU-H. (An oriented sample can only be made from PEU-H.) The resulting pinhole photograph (Figure 13) shows the presence of two meridian scatterings, which correspond to a *d* spacing of 36.5 and 18.1 Å, respectively. These values are approximately equal to those obtained above for PEU-L. The appearance of the well-oriented meridian scatterings confirmed the formation of a S_A mesophase for PEU. The *d* spacing evaluated from X-ray study (36.5 or 36.7 Å) corresponds to a nearly extended monomeric unit (Figure 14a). The deviation of the computed value (=41.1 Å, simulated from Chem3D) from the experimental one may be attributed to the single chain simulation, where no intermolecular H-bond interaction was considered in this calculation. It is reasonable to suggest that neighboring urethane and ester linkages are tied up by intermolecular H-bonds and result in the decrease of the chain dimension.

As concluded from the above study, PEUs actually possess a S_A mesophase. To achieve a S_A mesophase, the two aliphatic pentylene chains connected to the TDI-derived urethanes are supposed to align in an approximately parallel manner. (Therefore, these two connected pentylene chains are perpendicular to the smectic layer.) In this manner, the short-range translation motion occurs to enhance formation of intermolecular urethane−ester bond from an original urethane−urethane H-bond pair. The equal molar fractions of bonded external and urethane −C═O groups in the mesophase (as concluded from FTIR study) suggests that this transformation occurs easily during mesophase formation. This transition motion involves slippage of the chain segment over a distance of ~9 Å. An imperfect smectic A layered structure (Figure 14b), with certain portions of the mesogenic triads deviating from the smectic layer to have their inherent external ester −C═Os to bond with the urethane −NHs, is therefore proposed to account for the results from an infrared study.

Acknowledgment. This work was financially supported by The National Science Council, ROC, under Contract NSC84-2216-E-110-008.

References and Notes

(1) Coleman, M. M.; Graf, J. F.; Painter, P. C. *Specific Interacition and Miscibility of Polymer Blends*; Technomoic: Lancaster, PA, 1991.

(2) (a) Mormann, W.; Braham, M. *Makromol. Chem.* **1989**, *190*, 631. (b) Mormann, W.; Baharifar, A. *Polym. Bull.* **1990**, *24*, 413. (c) Mormann, W.; Braham, M. *Macromolecules* **1991**, *24*, 1096. (d) Diana, J. G.; Macosko, C. W. *Polym. Prepr.* **1992**, *33* (1), 1109. (e) Mormann, W.; Benadda, S. *Polym. Prepr.* **1993**, *34* (2), 739. (f) Mormann, W.; Braham, M. *Polymer* **1993**, *34*, 187. (g) Mormann, W.; Brahm, M. *Mol. Cryst. Liq. Cryst.* **1990**, *185*, 163.

(3) (a) Tanaka, M.; Nakaya, T. *Kobunshi Ronbunshu* **1986**, *43*, 311. (b) Tanaka, M. *Makromol. Chem.* **1986**, *187*, 2345. (c) Tanaka, M.; Nakaya, T. *J. Macromol. Sci., Chem.* **1987**, *A24*, 777. (d) Stenhouse, P. J.; Valles, E. M.; Kantor, S. W.; MacKnight, W. J. *Macromolecules* **1989**, *22*, 1467. (e) Lorenz, R.; Els, M.; Haulena, F.; Schmitz, A.; Lorenz, O. *Angew. Makromol. Chem.* **1990**, *180*, 51. (f) Lee, J. B.; Kato, T.; Yoshida, T.; Uryu, T. *Macromolecules* **1993**, *26*, 4989. (g) Sufiyama, K.; Shiraishi, K.; Kato, K. *Polym. J.* **1993**, *25*, 103. (h) Papadimtrakopoulos, F.; Hsu, S. L.; MacKnight, W. *Macromolecules* **1992**, *25*, 4671. (i) Papadimitrakopoulos, F.; Sawa, E.; MacKnight, W. J. *Macromolecules* **1992**, *25*, 4682. (j) Smyth, G.; Valles, E. M.; Pollack, S. K.; Grebowicz, J.;

Stenhouse, P. J.; Hsu, S. L.; MacKnight, W. J. *Macromolecules* **1990**, *23*, 3389. (k) Pollack, S. K.; Shen, D. Y.; Hsu, S. L.; Wang, Q.; Stidham, H. D. *Macromolecules* **1989**, *22*, 551. (l) Pollack, S. K.; Smyth, G.; Papadimitrakopoulos, F.; Stenhouse, P. J.; Hsu, S. L.; Macknight, W. J. *Macromolecules* **1992**, *25*, 2381. (m) Lee, J. B.; Kato, T.; Yoshida, T.; Uryu, T. *Macromolecules* **1993**, *26*, 4990. (n) Papadimitrakopoulos, F.; Sawa, E.; MacKnight, W. J. *Macromolecules* **1992**, *25*, 4682.

(4) Yang, F. S.; Hong, J. L. *Macromolecules* **1997**, *30*, 7927.

(5) Lin, C. H.; Hong, Y. L.; Yen, F. S.; Hong, J. L. *Liq. Cryst.* **1996**, *21*, 609.

(6) Brunette, C. M.; MacKnight, W. J. *Polym. Eng. Sci.* **1981**, *21*, 163.

(7) Brunette, C. M.; Hsu, S. L.; MacKnight, W. J. *Macromolecules* **1982**, *15*, 71.

(8) Galbiati, E.; Zerbi, G. *Polymer* **1991**, *32*, 1555.

(9) MacKnight, W. J.; Yang, M. *J. Polym. Sci., Symp.* **1973**, *42*, 817.

(10) Bulkin, B. J. In *Liquid Crystals: the Fourth State of Matter*; Saeva, F. D., Ed.; Marcel Dekker: New York, 1979; p 365.

(11) Song, C. S. P.; Schneider, N. S. *Macromolecules* **1975**, *8*, 68.

(12) Coleman, M. M.; Lee, K. H.; Skrovanck, D. J.; Painter, P. C. *Macromolecules* **1986**, *19*, 2149.

(13) Skrovanck, D. J.; Painter, P. C.; Coleman, M. M.; Lee, K. H. *Macromolecules* **1986**, *19*, 699.

(14) Skrovanck, D. J.; Howes, S. E.; Painter, P. C.; Coleman, M. M. *Macromolecules* **1985**, *18*, 1676.

(15) Coleman, M. M.; Skrovanck, D. J.; Howes, S. E.; Painter, P. C. *Macromolecules* **1985**, *18*, 299.

(16) Seymour, R. W.; Estes, G. M.; Cooper, S. L. *Macromolecules* **1970**, *3*, 579.

(17) Senich, G. A.; MacKnoght, W. J. *Macromolecules* **1980**, *13*, 106.

(18) Bhafwager, D. E.; Painter, P. C.; Coleman, M. M.; Krizan, T. D. *J. Polym. Sci., Polym. Phys.* **1991**, *29*, 1547.

(19) Moskala, E. J.; Howes, S. E.; Painter, P. C.; Coleman, M. M. *Macromolecules* **1984**, *17*, 1671.

(20) Garton, A. *Polym. Eng. Sci.* **1984**, *24*, 112.

(21) Maddams, W. F. *Appl. Spectrosc.* **1980**, *34*, 24.

(22) Boyarchuk, Y. M.; Rappoport, L. Y.; Nikitin, V. N.; Apukhtina, N. P. *Vysolomol. Soyed.* **1975**, *7*, 778.

MA9804186